LAMINAR AIR FLOW FREE CONVECTIVE HEAT TRANSFER INSIDE A VERTICAL CIRCULAR PIPE WITH DIFFERENT INLET CONFIGURATIONS

by

Hussein A. MOHAMMED and Yasin K. SALMAN

Original scientific paper
UDC: 536.25:532.517.2
BIBLID: 0354-9836, *11* (2007), 1, 43-63

Free convection heat transfer has been experimentally investigated for laminar air flow in a vertical circular pipe by using the boundary condition of constant wall heat flux in the ranges of local Rayleight number (Ra_L) from $1.1 \cdot 10^9$ to $4.7 \cdot 10^9$. The experimental setup was designed for determining the effect of different configurations placed at the inlet of a vertical heated pipe, on the surface temperature, the local and average heat transfer coefficients. The apparatus was made with an electrically heated aluminum pipe with length of 900 mm and inside diameter 30 mm. The inlet configurations included two circular pipes having the same diameter as the heated pipe but with lengths of 600 and 1200 mm, sharp-edge and bell-mouth. It was found that the surface temperature along the pipe surface for same heat flux would be higher values for inlet condition with length of 1200 mm and would be lower values for bell-mouth inlet condition. The results show that the local Nusselt number Nu_x and average Nusselt number ($\overline{Nu_L}$) values would be higher for bell-mouth inlet condition and lower values for 1200 mm inlet condition. For all inlet configurations, the results reveal that the Nu increases as the heat flux increases. Empirical correlations have been proposed in a form of log $\overline{Nu_L}$ vs. log $\overline{Ra_L}$ for each case investigated and a general correlation for all cases has been obtained which reveals the effect of inlet conditions existence on the free convection heat transfer process in a vertical circular pipe.

Key word: *laminar flow, free convective heat transfer, vertical pipe, sharp-edge, bell-mouth, different inlet configurations*

Introduction

Free convection is the easiest and most inexpensive way to cool the internal surfaces of vertical open-ended ducts and of tube banks, despite the low rates of heat transfer that this convection process affords. Thus, information on the behaviour of free convection flow through confines spaces has been found useful especially in the thermo-fluid systems encountered in the diverse fields of the storage of cryogenic fluids, nuclear engineering, and solar energy. Due to its importance, the free convection problem has received increasing attention in the literature in the past two decades [1]. The following an-

alytical and experimental studies, however, have mainly restricted their consideration on free convection for different fluids in a tube subjected to different boundary conditions, but the specific problem that will be considered here is that of constant wall heat flux. However, most of the available works deal with vertical tubes in special cases only. To authors knowledge the available work is scarce on the case, which studied in the present work. The present work has been carried out in an attempt to fill a part of the existing gap. It provides experimental data on uniformly heated constant wall heat flux in a vertical circular pipe with different inlet configurations. Meric [2] analyzed the development of free convection in finite vertical tubes by an analytical method, which is based upon a slug-flow linearization of the governing boundary-layer type equations. The resulting equations have been solved by means of Laplace transformations to give simple closed form expression for the flow variables. The variation of inlet velocity with Gr number, velocity and temperature profiles for Pr = 0.7 were depicted; also the fluid pressure distribution and heat flux *vs*. tube length were presented. The results have been compared with available numerical results and showed good agreement. Barrow [3] investigated theoretically and experimentally upward free convection for air (Pr = 0.7) in an internally heated vertical duct open at both ends. The experimental data for the wall temperature distribution and local heat transfer coefficient have been compared with the results of numerical analysis of an idealized and laminar flow heat transfer model. Correlations for the average Nusselt number, maximum wall temperature and flow rate were presented with the Rayleigh number as the independent variable. Kokugan and Kinoshita [4] performed an experimental work in a heated vertical open tube at constant wall temperature. Correlations between Gr and Re numbers have been derived by setting up a mechanical energy balance in the tube. The following equation has been obtained as:

$$\mathrm{Gr}_0 \quad 6.3\,\mathrm{Re}_0^2 \quad \frac{3.2(L_\mathrm{H} \quad L_0)}{D\,\mathrm{Re}_0} \tag{1}$$

where L_H is the heated length, L_0 is the entrance length, and subscript (0) denoted to at room temperature. The results have been compared with available numerical results and showed good agreement. Hess and Miller [5] carried out experiments using a laser-Doppler velocitymeter (LDV) to measure the axial velocity of a fluid contained in a cylinder subject to constant heat flux on the side walls. The modified Rayleigh numbers ranged between $4.5\cdot10^9$ to $6.4\cdot10^{10}$, which corresponds to the upper limit of the laminar regime. The flow field inside the boundary layer has been divided into three regions along the axis of the cylinder and a parabolic distribution has been used to fit the data within each region. Variations of axial velocity with radius for different height in the bottom and top parts of the cylinder and inside the boundary layer region and with radius for different time were presented. The variation of radial position of maximum velocity and radial position of zero velocity with Rayleigh number was depicted. Excellent agreement has been found with an available numerical solution. Shigeo and Adrian [6] studied experimentally natural convection in a vertical pipe with $L/D = 9$ for different end temperature. The Rayleigh number based on diameter was in the range of $10^8 < \mathrm{Ra}_\mathrm{D} < 10^{10}$. It was concluded that the natural convection mechanism departs considerably from the pattern known in the limit

Ra 0. In each vertical cross-section, the top-bottom temperature difference is of the same order of magnitude as the end-to-end temperature difference. The Nusselt number for end-to-end heat transfer was shown to vary weakly with the Rayleigh number. Shenoy [7] presented a theoretical analysis of the effect of buoyancy on the heat transfer to non-Newtonian power-law fluids for upward flow in vertical pipes under turbulent conditions. The equation for quantitative evaluation of the natural convection effect on the forced convection has been suggested to be applicable for upward as well as downward flow of the power-law fluids by a change in the sign of the controlling term. Chang *et al*. [8] investigated theoretically the role of latent heat transfer in connection with the vaporization of a thin liquid film inside vertical tube, in natural convection flows driven by the simultaneous presence of combined buoyancy effects of thermal and mass diffusion. The effects of tube length and system temperatures on the momentum, heat and mass transfer in the flow have been examined. The important role that the liquid film plays under the situations of buoyancy-aiding and opposing flows was clearly demonstrated. Al-Arabi *et al*. [9] investigated experimentally natural convection heat transfer from the inside surfaces of vertical tubes to air in the ranges of $Gr_L Pr$ from $1.44 \cdot 10^7$ to $1.02 \cdot 10^{10}$ and *L/D* ranged from 10 to 31.4. The results obtained have been correlated by dimensionless groups as follows:

$$Nu_{mL} \quad \frac{1.11}{1 \quad 0.05(t_{ms} \quad t_i)} (Gr_{mL} Pr)^{0.25} \tag{2}$$

In this study, the effect of *L/D* on Nu_{mL} was insignificant and the entrance length was practically constant. The results have been compared with the available theoretical data and showed good agreement. Abd-el-Malek and Nagwa [10] developed an analysis of transformation group method to study fluid flow and heat transfer characteristics for steady laminar free convection on a vertical circular cylinder. The system of ordinary differential equations has been solved numerically using a fourth-order Runge-Kutta scheme and the gradient method. The effects of the cylinder heating mode and the Prandtl number on the velocity and temperature profiles have been investigated. It has been found that the maximum value of the vertical component of the velocity decreases with the increase of both the Prandtl number and the surface temperature. Fukusako and Takahashi [11] investigated the influence of density inversions and free convection heat transfer of air-water layers in a vertical tube with uniformly decreased wall temperature. Holographic interferometry was adopted to determine the time-dependent temperature distribution in the tube. The temperature, the flow patterns and the heat transfer characteristics along the tube wall have been determined. Yan and Lin [12] performed combined theoretical and experimental study to investigate natural convection in a vertical pipe flows at high Rayleigh number. The wall conduction effects and thermal property variations of the fluid and pipe wall were also considered. A low-Reynolds-number turbulence model has been employed to treat the transitional and turbulent flow regimes including buoyancy effects. The predicted and measured distributions of wall temperature and Nusselt number were in good agreement. Vinokurov *et al*. [13] carried out an experimental investigation of unsteady-state free convection in a vertical cylindrical channel

for the case of non-uniform distribution of heat flux along the channel at a constant wall temperature. The averaged temperature field in a gas has been investigated on a Mach-Zender interferometer. Hydrodynamic structures have been investigated by the smoke visualization technique. Longitudinal and lateral Rayleigh numbers were varied from 0 to $4\cdot10^9$ and from $0.8\cdot10^4$ to$1.2\cdot10^5$, respectively. Investigations have been carried out with air, carbon dioxide, and helium flows as working fluids. Yissu [14] examined numerically and experimentally the problem of laminar natural convection in vertical tubes with one end open to a large reservoir, designated open thermosyphon, to predict flow behavior and the heat transfer rates. In the numerical study, a semi-implicit, time-marching, finite-volume solution procedure has been adopted to solve the three governing equations mass, momentum, and energy sequentially. Experimental work involved the use of a Mach-Zehnder interferometer to examine the temperature field for a modified rectangular open thermosyphon through the interpretation of fringe patterns. Nusselt numbers have been determined from the interferometer results and compared with numerical results. Kuan-Tzong [15] presented a closed form solution for fully developed laminar natural convection heat and mass transfer in a vertical partially heated circular duct. Thermal boundary conditions of uniform wall temperature / uniform wall concentration (UWT/UWC) and uniform heat flux / uniform mass flux (UHF/UMF) have been considered. Wojciech [16] presented experimental and numerical studies for natural convection in a vertical tube placed between two isothermal walls of different temperature. Two experimental setups were built for visualizing the flow and to measure the temperature around the tube and walls confined in the close cavity. An FEM computer code has been applied for analyzing the influence of various parameters on the flow structure and heat transfer. The fluid in slot is air (Pr = 0.71). The measurements have been taken for Rayleigh number: for slot $Ra_s = 2\cdot10^7 - 1\cdot10^9$; for tube $Ra_r = 6\cdot10^2 - 9\cdot10^2$. It has been observed that the hot air near the heated wall aspirated the layers of hot air from the vertical tube. He *et al*. [17] investigated numerically natural convection heat transfer and fluid flow in a vertical cylindrical envelope with constant but different temperatures of the two end surfaces and an adiabatic lateral wall. The simulation has been conducted for two end wall temperature differences: $T_w = 10$ and 220 K and with the range of $Ra_L = 1.1\cdot10^5$ to $4\cdot10^7$. For the cases of $T_w = 10$ K, it was found that the variation patterns of Nu_L *vs*. Ra_L within the range of $L/D = 3$-10 were in good consistency with the available experimental and theoretical results. Numerical simulation also revealed that the ratio of the axial length, L, to the diameter, D, has effect on the average heat transfer rate of the envelope under the same other conditions. Within the range of $L/D = 1$-9, the increase in L/D leads to decrease in heat transfer rate. Moawed [18] studied experimentally natural convection from uniformly heated helicoidal pipes oriented vertically and horizontally. The effects of pitch to pipe diameter ratio, coil diameter to pipe diameter ratio and length to pipe diameter ratio on the average heat transfer coefficient have been examined. The experiments covered a range of Ra number based on tube diameter from $1.5\cdot10^3$ to $1.1\cdot10^5$. The results show that the overall average Nusselt number, Nu_m, increases with the increase in pitch to pipe diameter ratio, coil diameter to pipe diameter ratio, and length to pipe diameter ratio for vertical helicoidal pipes. The above literature survey clearly indicates the lack of studies on natural convection from the inside surface of a vertical tube with differ-

ent configurations placed at the inlet of a vertical circular tube. Therefore, the purpose of the present study is to provide experimental data on free convection laminar air heat transfer from open ended vertical circular pipe with a constant wall heat flux boundary condition and with different inlet configurations and to propose empirical correlations for this problem.

Experimental apparatus

The experimental apparatus was designed to have a heated section preceded with different inlet conditions having different configurations and lengths, as well as, different Grashof number is shown schematically in fig. 1, to investigate natural convection heat transfer in a vertical circular pipe. The apparatus consists of a cylindrical heated section open at both ends, mounted vertically on a wooden board and the lower end of the inlet configuration is protected from outside air currents by nylon shields (7).

Test pipe and thermocouples installation

The heated pipe (4) provided with changeable inlet conditions with four different configurations, particulars of which are: cylindrical pipes with lengths of 600 mm (L/D = 20), 1200 mm (L/D = 40), sharp-edge, and bell-mouth. The air was withdrawn from atmosphere flows due to buoyancy effect through the different inlet conditions, enters then into the heated pipe and the heated air was exhausted to the atmosphere. The heated pipe (4) was made of aluminum pipe with 30 mm inside diameter, 35 mm outside

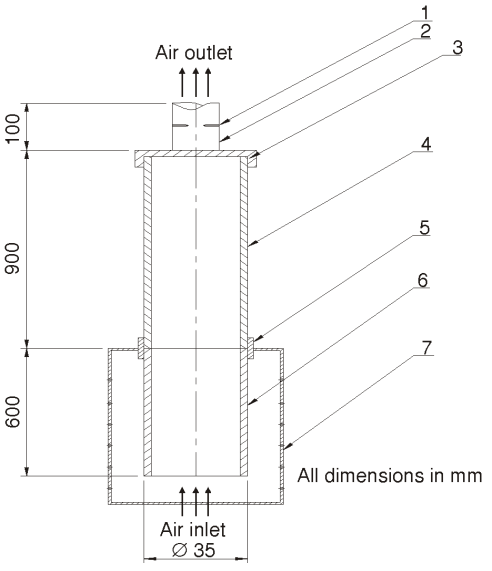

Figure 1a. Layout of experimental setup shows the inlet restriction with L/D = 20
1 – thermocouples, 2 – mixing chamber, 3 – exit teflon piece, 4 – circular heated section, 5 – teflon connection piece, 6 – calming section, 7 – nylon shields

diameter and 900 mm length. To provide a fully developed velocity profile at the entrance of the heated pipe, the flow passed through cylindrical pipes (calming sections) (6) having the same diameter as the heated pipe but with variable lengths, one with of 600 mm as shown in fig.1a, and the other with length of 1200 mm. These entrance pipes were connected with the heated pipe by using a teflon connection piece (5) bored with the same inside diameter of the heated pipe and the entrance pipes calming section pipe as shown in fig.1a and it represents a part of the heated pipe inlet, with 30 mm inside diameter, 50 mm outside diameter, and 80 mm long. Another teflon piece represents the heated pipe exit (3) and it has dimensions of 30 mm inside diameter, 88 mm outside diameter and 25 mm long. The teflon was chosen because its low thermal conductivity in order to reduce the test section ends losses. To provide a uniform velocity profile at the entrance of the heated pipe, the flow passed through a honeycomb flow straightener (5), as shown in fig.1b, placed inside a well designed nozzle bell-mouth (6), with a total length of 250 mm and had a contraction ratio of 3 as shown in fig. 1b, and was constructed from teflon to reduce the flow fluctuations and to get a uniform flow at the heated pipe entrance. The bell-mouth was fitted at the aluminum heated pipe. The sharp--edged entrance, as shown in fig. 1c, was simulated by using a circular teflon piece fitted (5) at the entrance of the heated pipe and it has 30 mm inside diameter and 50 mm outside diameter with length of 100 mm. The pipe is heated electrically by using an electrical heater (3) as shown in fig. 1d. It consists of nickel-chrome wire electrically isolated by ceramic beads, wounded uniformly along the pipe as a coil in order to give uniform wall heat flux. An asbestos rope was used as spacer to secure the winding pitch. The outside of the test section was then thermally insulated by using asbestos (4) and fiberglass layers (5), having thicknesses of 15 mm and 16 mm, respectively. Twenty--five 0.2 mm asbestos sheath copper-constantan (type T) thermocouples (2), were used to measure the pipe surface temperatures along the pipe surface. The thermocouples were fixed by drilling

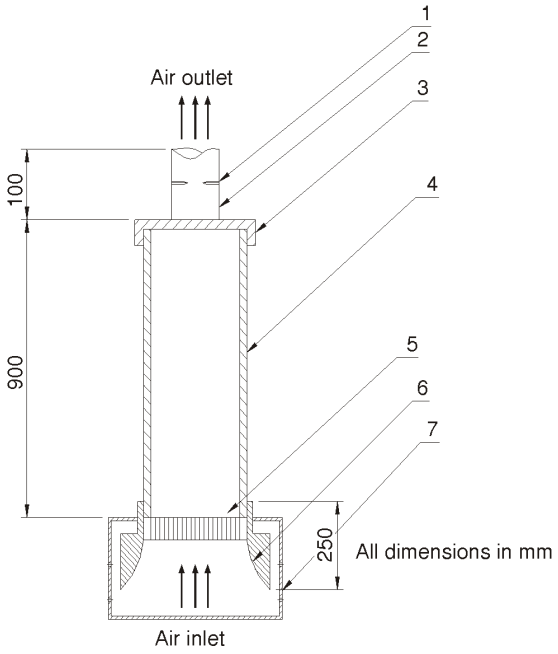

Figure 1b. Layout of experimental setup shows the inlet restriction with bell-mouth
1 – thermocouples, 2 – mixing chamber, 3 – exit teflon piece, 4 – circular heated section, 5 – honeycomb straightener, 6 – inlet bell-mouth teflon piece, 7 – nylon shields

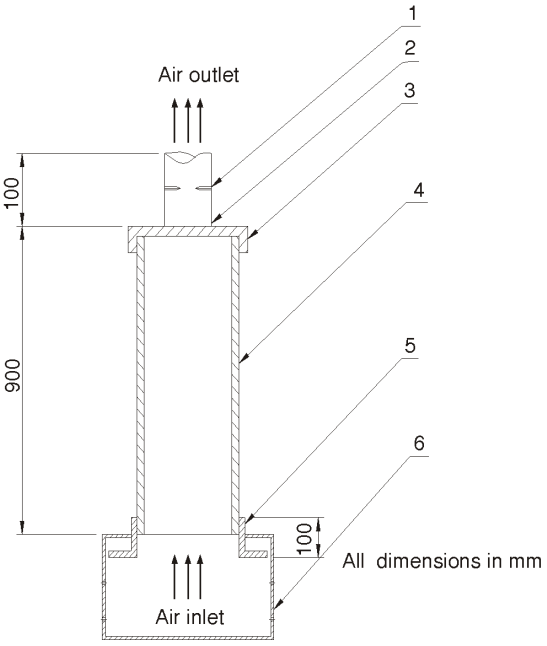

Figure 1c. Layout of experimental setup shows the inlet restriction with sharp-edge
1 – thermocouples, 2 – mixing chamber, 3 – exit teflon piece, 4 – circular heated section, 5 – inlet sharp-edge teflon piece, 6 – nylon shields

twenty five holes and along the pipe wall. The measuring junctions (which were made by fusing the ends of the wires together by means of an electric spark in an atmosphere free from oxygen) embedded in grooves in the wall normal to the pipe axis as shown in fig. 1d. The measuring junctions were secured permanently in the holes by sufficient amount of high temperature application defcon adhesive. All thermocouples were used with leads and calibrated using the melting points of ice made from distilled water as reference point and the boiling points of several pure chemical substances. The inlet bulk air temperature was measured by one thermocouple

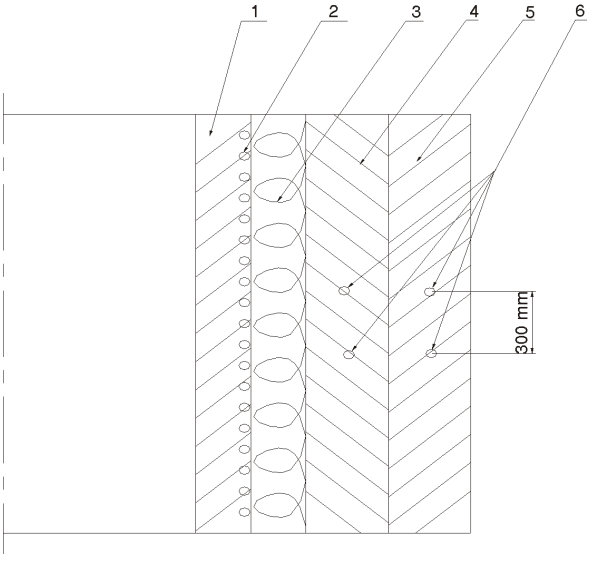

Figure 1d. Schematic diagram of heating element
1 – circular heated tube, 2 – surface thermocouples, 3 – electrical heater, 4 – asbestos layer, 5 – fiberglass layer, 6 – thermocouples of lagging

placed in the beginning of the different inlet condition, while the outlet bulk air temperature was measured by two thermocouples (1) located in the heated section exit "mixing chamber" (2) as shown in fig. 1a, fig. 1b, and fig. 1c, respectively. The local bulk air temperature was calculated by fitting straight line-interpolation between the measured inlet and outlet bulk air temperatures. The heat loss through the heated section lagging, could be calculated by inserting six thermocouples (6) in the lagging as two thermocouples at three stations along the heated section as shown in fig. 1d. By using the average measured temperatures and thermal conductivity of the lagging, the heat loss through lagging can be determined. The heat losses from the ends of the heated section could be evaluated by inserting two thermocouples in each teflon piece. By knowing the distance between these thermocouples and the thermal conductivity of the teflon, the end losses could be calculated.

Experimental procedure

The voltage regulator (variac), accurate ampermeter and digital voltmeter have been used to control and measure the input power to the working pipe. The apparatus has been allowed to turn on for at least 4 hours before the steady-state condition was achieved. The readings of all thermocouples have been recorded every half an hour by a digital electronic thermometer until the reading became constant, and then the final reading has been recorded. The input power to the heater could be changed to cover another run in shorter period of time and to obtain steady-state conditions for next heat flux.

Uncertainty analysis

In the present work, the uncertainties in heat transfer coefficient (Nusselt number) and Rayleigh number have been estimated following the differential approximation method as reported by Holman [19]. For a typical experiment, the total uncertainty in measuring the heater input power, temperature difference ($T_s - T_a$), the heat transfer rate and the circular pipe surface area were 0.37%, 0.47%, 2.5%, and 1.4%, respectively. These were combined to give a maximum error of 2.38% in heat transfer coefficient (Nusselt number) and maximum error of 2.14% in Rayleigh number.

Data analysis method

The main independent parameter in these experiments is the Grashof number (controlled by the input power). After adjusting the desired value of the heat input to the heated pipe, the experiments were allowed to run for at least four hours before steady--state condition was established. Once the steady-state was attained, the readings of thermocouples, input power, and the flux meter (for heat losses through the insulation) were recorded. The natural convection heat transfer process for air flow in a vertical circular pipe when its surface was subjected to a constant wall heat flux boundary condition has been analyzed.

The convection heat transferred from the heated pipe surface could be calculated as:

$$Q_{conv} = Q_t - Q_{cond} - Q_{rad} \quad (3)$$

The total input power supplied to the heated pipe can be calculated from:

$$Q_t = VI \quad (4)$$

Q_{cond} is the total conduction heat losses (lagging and ends losses) and its calculated from:

$$Q_{cond} \quad \frac{\Delta T}{R_{th}} \quad (5)$$

where R_{th} is the thermal resistance of the insulations. The conduction heat losses from the heated section are approximately about 4%.

The radiation heat transfer from the heated pipe could be calculated from this analysis: firstly the interior surfaces and the bottom of the pipe might be deemed as black bodies but the outer surface of the heated pipe is thermally insulated. Secondly, after assuming the interior surface as surface A1, the bottom of the pipe as surface A2, and the top surface of the pipe as surface A3, as shown in fig. 1e, the radiative heat transfer equation could be calculated as follows:

$$Q_{rad} \quad A_1\sigma F_{13}(T_1^4 \quad T_3^4) \quad A_2\sigma F_{23}(T_2^4 \quad T_3^4) \quad (6)$$

where A_1 is the surface area of the pipe, = DL, A_2 is the cross-sectional area of the pipe, = (D^2, F_{13} is the shape factor between the surfaces 1 and 3, F_{23} is the shape factor between the surfaces 2 and 3, and σ is the Stefan-Boltzmann constant.

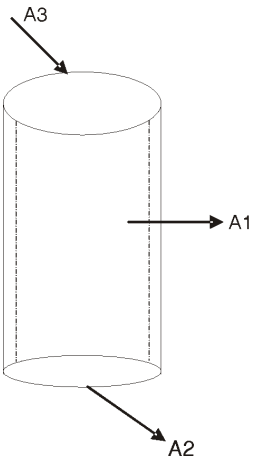

Figure 1e. The considered radiation surfaces of the heated pipe

In addition the shape factor of the surfaces could be evaluated as follows.

After evaluate the values of the dimensional ratios of (r_i/L) and (L/r_i), (where r_i is the inner radius of the pipe) then the value of F_{23} could be calculated from fig. 15.3 as reported by Incropera and DeWitt [1]:

$$F_{21} = 1 - F_{23} \quad (7)$$

$$F_{12} \quad \frac{A_2}{A_1} F_{21} \quad (8)$$

$$F_{13} = F_{12} \quad (9)$$

After calculating the radiative heat transfer from the pipe it was noticed that its very small compared with the total heat transfer and conduction heat transfer, and consequently it could be ignored.

The convection heat flux can be obtained from:

$$q_{\text{conv}} \quad \frac{Q_{\text{conv}}}{A_{\text{s}}} \tag{10}$$

where $A_{\text{s}} = \pi DL$

The convection heat flux, which is used to calculate the local and average heat transfer coefficient, is as follows:

$$h_{\text{x}} \quad \frac{q_{\text{conv}}}{T_{\text{sx}} \quad T_{\text{bx}}} \tag{11}$$

where T_{sx} is the local surface temperature and T_{bx} is the local bulk air temperature.

All the air properties have been evaluated at the mean film temperature as reported in Incropera and DeWitt [1]:

$$T_{\text{fx}} \quad \frac{T_{\text{sx}} \quad T_{\text{bx}}}{2} \tag{12}$$

where T_{fx} is the local mean film air temperature.

The local Nusselt number can be determined as:

$$\text{Nu}_{\text{L}} \quad \frac{h_{\text{x}} L}{k} \tag{13}$$

The average values of Nusselt number can be calculated based on the average heat transfer coefficient as follows:

$$\overline{h_{\text{L}}} \quad \frac{1}{L} \int_{x\ 0}^{x\ L} h_{\text{x}}\,\text{d}x \tag{14}$$

$$\overline{\text{Nu}_{\text{L}}} \quad \frac{\overline{h_{\text{L}}} L}{k} \tag{15}$$

The average values of the surface temperature, bulk air temperature, and mean film temperature can be evaluated as follows:

$$\overline{T_{\text{s}}} \quad \frac{1}{L} \int_{x\ 0}^{x\ L} T_{\text{sx}}\,\text{d}x \tag{16}$$

$$\overline{T_{\text{a}}} \quad \frac{1}{L} \int_{x\ 0}^{x\ L} T_{\text{bx}}\,\text{d}x \tag{17}$$

$$\overline{T_f} \quad \frac{\overline{T_s} \quad \overline{T_a}}{2} \tag{18}$$

where $\beta = 1/273 + \overline{T_f}$. All the air physical properties (ρ, μ, ν, and k) in the present work have been evaluated at the average mean film temperature $\overline{T_f}$, but all the physical properties in the previous papers which listed in references have been taken at the mean film temperature which based on ambient temperature at pipe entrance and given by $T_{mf} = (T_{ms} + T_i)/2$ as reported by Al-Arabi *et al*. [9].

Result and discussion

A total of 28 test runs have been conducted to cover four inlet conditions with different lengths and configurations of circular pipes (calming sections) with length of 600 mm ($L/D = 20$), 1200 mm ($L/D = 40$), sharp-edge, and bell-mouth. The range of heat flux is varied from 249 to 1000 W/m^2.

Surface temperature

Generally, many variables such as heat flux, and the flow inlet condition situation may affect the variation of the surface temperature along the pipe. The surface temperature distribution for selected runs is plotted in figs. 3-6. The distribution of the surface temperature (T_s) with pipe axial distance for all inlet conditions has the same general shape. This behaviour can be explained if fig. 2 is considered, at the pipe entrance (point a) the surface temperature increases since the thickness of the boundary layer is zero. Then it gradually increases until reach a maximum value at point b due to the axial conduction and the transition from laminar to turbulent flow, and also the boundary layer fills the pipe. From point a to point b the heat transfer gradually decreases and T_s gradually increases. Beyond the maximum point (point b) the surface temperature is decreased due to the laminarization effect in the near wall region (buoyancy effect) and due to pipe end losses. In addition, one would surmise a straight-line (T_s-x) relation b-c is the case being that of con-

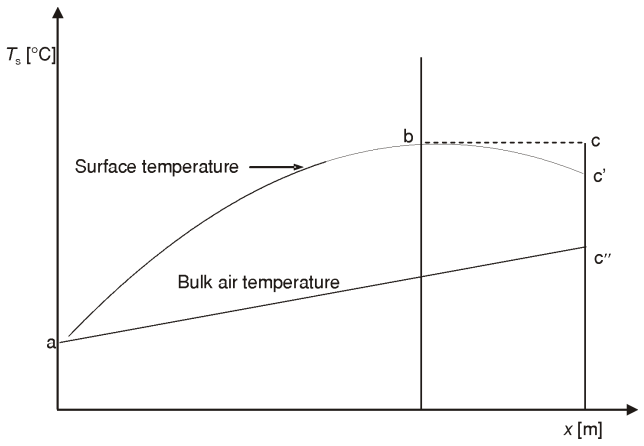

Figure 2. Variation of the surface temperature and the bulk air temperature *vs.* axial distance along the pipe

stant wall heat flux. However, as the air is heated along the pipe, its physical properties gradually change with the increased temperature. The thermal conductivity increases causing less resistance to the flow of heat and the viscosity increases causing radial flow of the hotter layers of air nearer to the surface to the pipe center. A gradual increase of the local heat transfer beyond point b must then be appeared. For constant wall heat flux this can only take place if the local difference between the bulk air temperature (as shown by straight-line a-c") and the surface temperature decreases resulting in the shape of the (T_s-x) curve (a-b-c') as shown in fig. 2. Figure 3 shows the distribution of the surface temperature along the pipe for different heat fluxes, for inlet condition with length of 600 mm (L/D = 20). This figure reveals that the surface temperature increases at pipe entrance to reach a maximum value after which the surface temperature decreases. This also can be attributed to the developing of the thermal boundary layer faster due to buoyancy effect as the heat flux increases, and as elucidated previously. Figure 4 is similar to fig. 3 but pertains to inlet condition with length of 1200 mm (L/D = 40). The curves in the two figures show similar trend, but the surface temperature values in fig. 4 would be higher than that observed in fig. 3 due to the length of inlet condition. Figures 5 and 6 are similar in trends to figs. 3 and 4 but pertain to inlet conditions of sharp-edge and bell-mouth, respectively, which show lower surface temperature than that observed in figs. 3 and 4. Figures 7 and 8 show the effect of different inlet configurations on the pipe surface temperature for low heat flux 249 W/m^2 in fig. 7 and for high heat flux 996 W/m^2 in fig. 8. It is obvious from these figures that the increasing of inlet condition length causes to increase the surface temperature, as the heat flux is kept constant. It is necessary to mention that the friction between the inside surface of the inlet condition and the air flowing through it caused the temperature to be higher than the ambient temperature. It is also apparent from

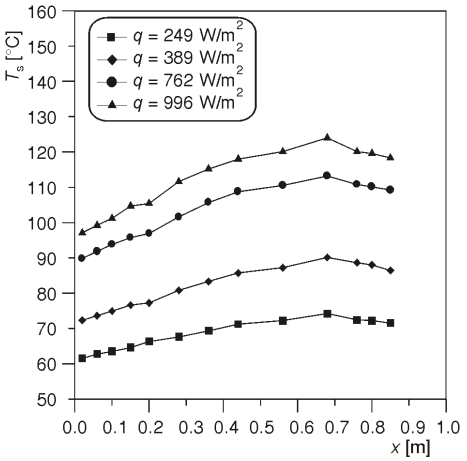

Figure 3. Variation of the surface temperature *vs.* the axial distance for L/D = 20

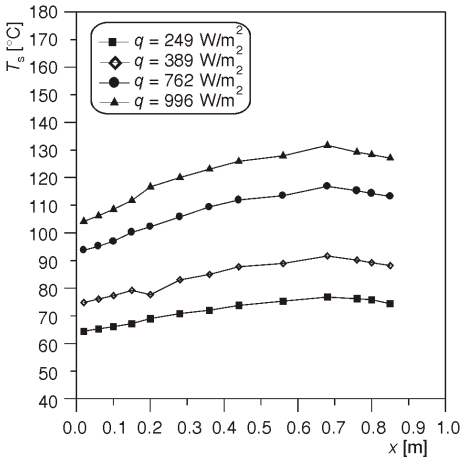

Figure 4. Variation of the surface temperature *vs.* the axial distance for L/D = 40

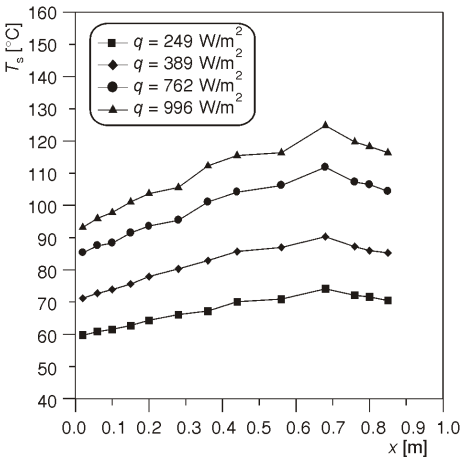

Figure 5. Variation of the surface temperature *vs.* the axial distance for sharp-edge

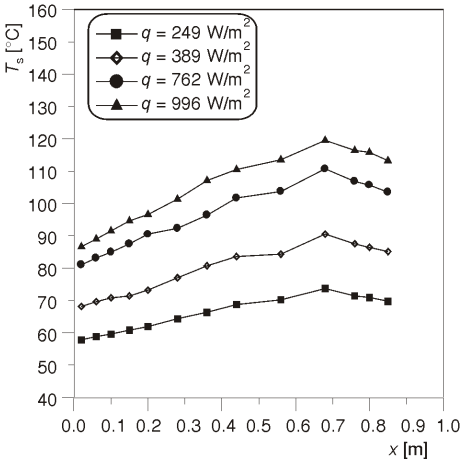

Figure 6. Variation of the surface temperature *vs.* the axial distance for bell-mouth

these figures that the lower values of the surface temperature take place in bell-mouth inlet configuration since the mass flow rate through the experimental pipe is the main parameter influencing the heat transfer results, so in bell-mouth inlet configuration which gives smallest flow resistance and maximal mass flow rate and finally lower surface temperature. It is also necessary to mention in the case of the configurations with unheated

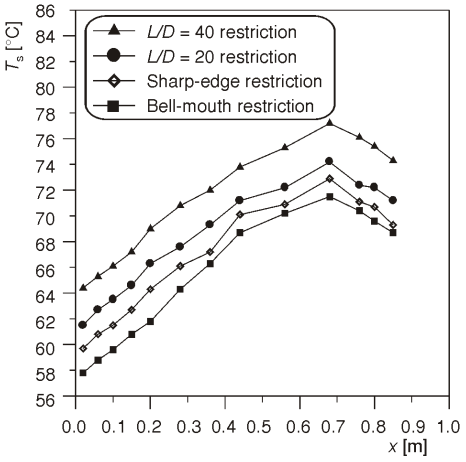

Figure 7. Variation of the surface temperature *vs.* the axial distance for different inlet configurations for q = 249 W/m^2

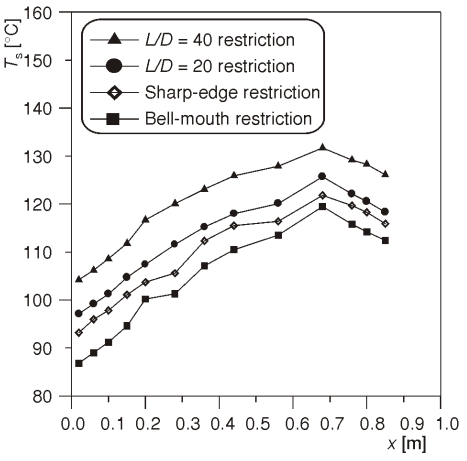

Figure 8. Variation of the surface temperature *vs.* the axial distance for different inlet configurations for q = 966 W/m^2

section $L/D = 20$ and $L/D = 40$ that the hydrodynamic boundary layer is developing before the thermal boundary layer and the flow would be thermally developing since the velocity profile is fully developed at the entrance of the heated pipe. But, in the case of bell-mouth inlet configuration, the hydrodynamic and thermal boundary layers are simultaneously developing and the flow at the entrance of the heated pipe has uniform velocity profile and for this inlet the boundary layer along the tube wall is at first laminar and then changes through a transition to turbulent condition. Therefore, it would be surmised that after specific axial distance of the heated pipe the boundary layers thickness (for hydrodynamic and thermal boundary layers) fulfils the pipe cross-section at approximately $x = 680$ mm since the maximum temperature for all inlet configurations takes place at this distance.

Local Nusselt number Nu_x

For free convection from a uniformly heated surface of length (L) exposed directly to the atmosphere, the mean heat transfer coefficient for the whole length is calculated from:

$$h_m = \frac{1}{L}\int_0^L h_x \, dx \tag{19}$$

where

$$h_x = \frac{q}{\Delta T} = \frac{q}{T_{sx} - T_{bx}} \tag{20}$$

ΔT in eq. 20 has been taken as the difference between the local surface temperature (T_{sx}) and the air temperature far away the effect of the surface. All previous investigators have calculated the heat transfer coefficient based on the temperature difference between the surface temperature and the fluid temperature at the entrance T_i (*i. e.* $\Delta T = T_{sx} - T_{bi}$). But, in the present work, since the heat transfer surface is not exposed to the atmosphere (because the flow is confined), so that the heat is transferred from the hot surface of the pipe to the air flowing in it. Therefore, $(\Delta T)_x$ cannot be taken equal to $T_s - T_i$. It should be taken as $T_{sx} - T_{bx}$ where T_{bx} is the local bulk air temperature of the pipe. The distribution of the local Nusselt number with the dimensionless axial distance X/D, is plotted for selected runs in figs. 9-14. Figures 9-12 show the effect of the heat flux variation on the Nu_x distribution for four inlet configurations which have been used in the present work. It is obvious from these figures that at higher heat flux, the results of Nu_x would be higher than the results of lower heat flux. This may be attributed to the secondary flow effect which increases as the heat flux increases leading to higher heat transfer coefficient. Therefore, as the heat flux increases, the fluid near the wall becomes hotter and lighter than the bulk fluid in the core. As a consequence, two upward currents flow along the sides walls, and by continuity, the fluid near the pipe center flows downstream. Figures 13 and 14 show the effect of different inlet configurations on the Nu_x distribution with X/D, for low heat flux 249 W/m^2 and for high heat flux 996 W/m^2, respectively. For constant heat flux, the Nu_x results would be higher values for bell-mouth inlet configuration and would be lower val-

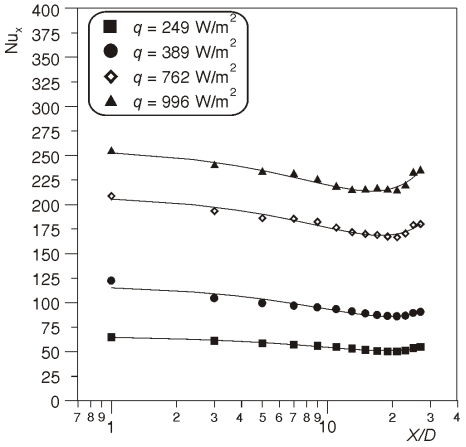

Figure 9. Variation of local Nusselt number *vs.* the dimensionless axial distance for *L/D* = 20

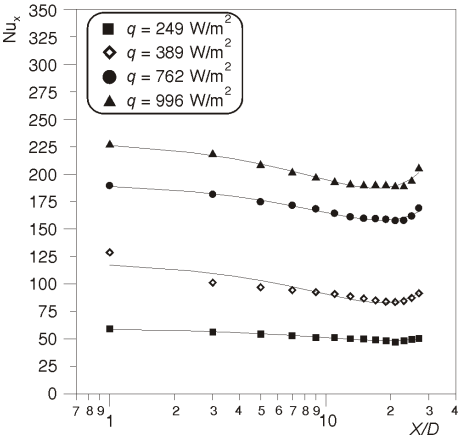

Figure 10. Variation of local Nusselt number *vs.* the dimensionless axial distance for *L/D* = 40

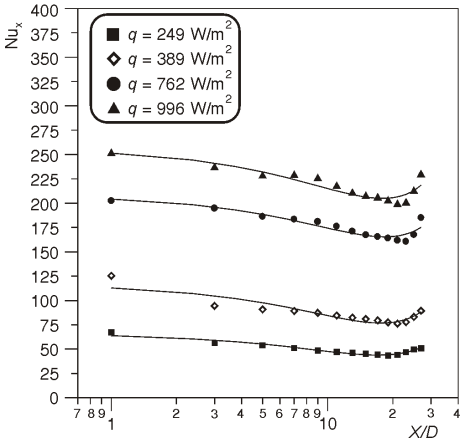

Figure 11. Variation of the local Nusselt number *vs.* the dimensionless axial distance for sharp-edge

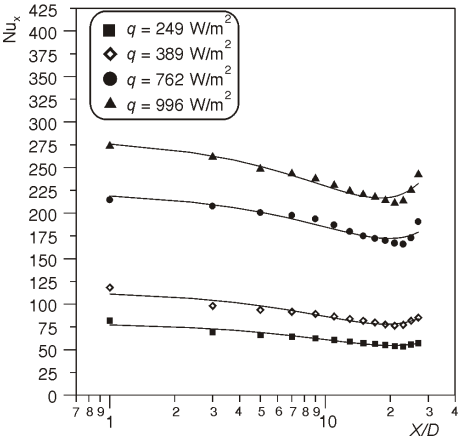

Figure 12. Variation of the local Nusselt number *vs.* the dimensionless axial distance for bell-mouth

ues for the configuration with $L/D = 40$. This situation reveals that in bell-mouth the velocity of flow is uniform and the intensity of turbulence is smaller than that in sharp-edge inlet condition since sharp-edge stimulate laminar to turbulence transition and gives higher turbulence intensity as a result of which the effect of viscosity becomes negligible. But for the

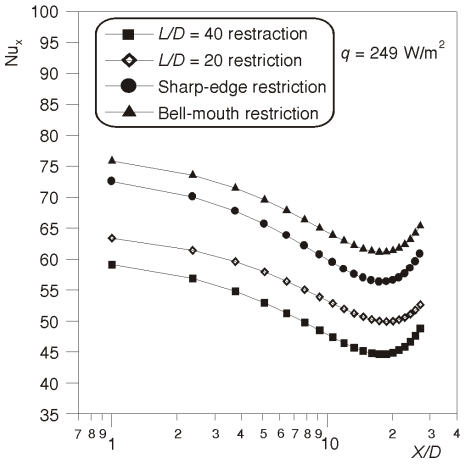

Figure 13. Variation of the local Nusselt number *vs.* the dimensionless axial distance for different inlet configurations

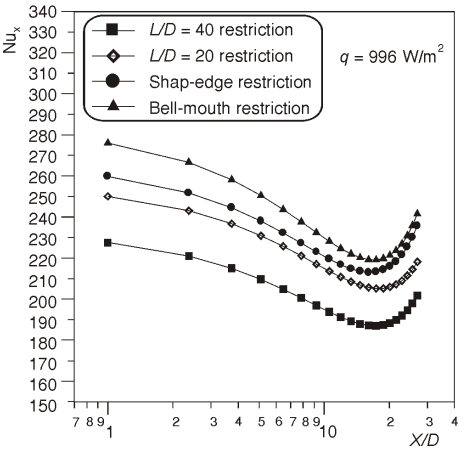

Figure 14. Variation of the local Nusselt number *vs.* the dimensionless axial distance for different inlet configurations

inlet conditions with lengths of $L/D = 20$ and $L/D = 40$, the velocity profile in these conditions are fully developed at the pipe entrance that may be becomes as a resistance on the flow and as L/D is higher the resistance would be higher, so that the surface temperature as a consequence would be higher, this leads to lower values of Nu_x than that for other inlet configurations. Finally, the mass flow rate through the experimental pipe which is the main parameter influencing heat transfer results, causes the maximum heat transfer would be in the bell-mouth inlet configuration, which gives smallest flow resistance and maximal mass flow rate. The present results, specifically for the cases of using different entrance pipes (calming sections) with $L/D = 20$ and $L/D = 40$, are qualitatively consistent with the observations given by He *et al.* [17] since the heat transfer decreases as L/D increases.

Average Nusselt number

The variation of the average Nusselt number ($\overline{Nu_L}$) with the dimensionless axial distance X/D is depicted for selected runs in figs. 15 and 16, which show the effect of the heat flux variation on the $\overline{Nu_L}$ for different inlet configurations for low heat flux 249 W/m^2 and high heat flux 996 W/m^2. The $\overline{Nu_L}$ variations for all configurations has similar trend as mentioned for Nu_x.

Average heat transfer correlation

The general correlation obtained from dimensional analysis by Incropera and DeWitt [1] for heat transfer by free convection is:

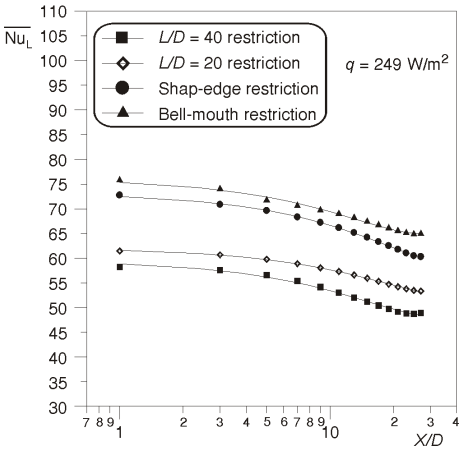

Figure 15. Variation of the average Nusselt number *vs.* the dimensionless axial distance for different inlet configurations

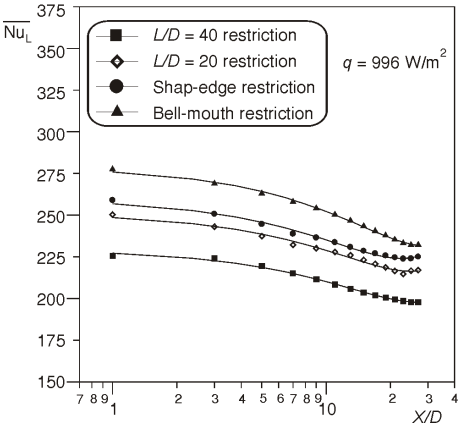

Figure 16. Variation of the average Nusselt number *vs.* the dimensionless axial distance for different inlet configurations

$$\overline{Nu} \quad f_1(\overline{Gr, Pr})^n \tag{21}$$

In the case of heat transfer from the inside surface of vertical pipes one expects that there is an effect of both length and diameter. For similarity with flat surface (which a cylinder of infinite diameter) the characteristic linear dimension in Nu and Gr may be taken as the cylinder length (L) since the circular pipe is vertically oriented in the present work. Then eq. (21) becomes:

$$\overline{Nu_L} \quad f_2(\overline{Gr_L, Pr})^n \tag{22}$$

Therefore, the following correlations have been obtained from the present work for each inlet configuration and a general correlation for all configurations has been proposed and the overall accuracy of heat transfer data in all these correlations is expected to be of the order of 8% as shown in fig.17:

$$\overline{Nu_L} \quad 1.176\overline{Ra_L}^{0.23} \quad \text{for configuration with } L/D = 40 \tag{23}$$

$$\overline{Nu_L} \quad 1.202\overline{Ra_L}^{0.23} \quad \text{for configuration with } L/D = 20 \tag{24}$$

$$\overline{Nu_L} \quad 1.372\overline{Ra_L}^{0.23} \quad \text{for sharp-edge configuration} \tag{25}$$

$$\overline{Nu_L} \quad 1.462\overline{Ra_L}^{0.23} \quad \text{for bell-mouth configuration} \tag{26}$$

$$\overline{Nu_L} \quad 1.248\overline{Ra_L}^{0.23} \quad \text{for all inlet configurations} \tag{27}$$

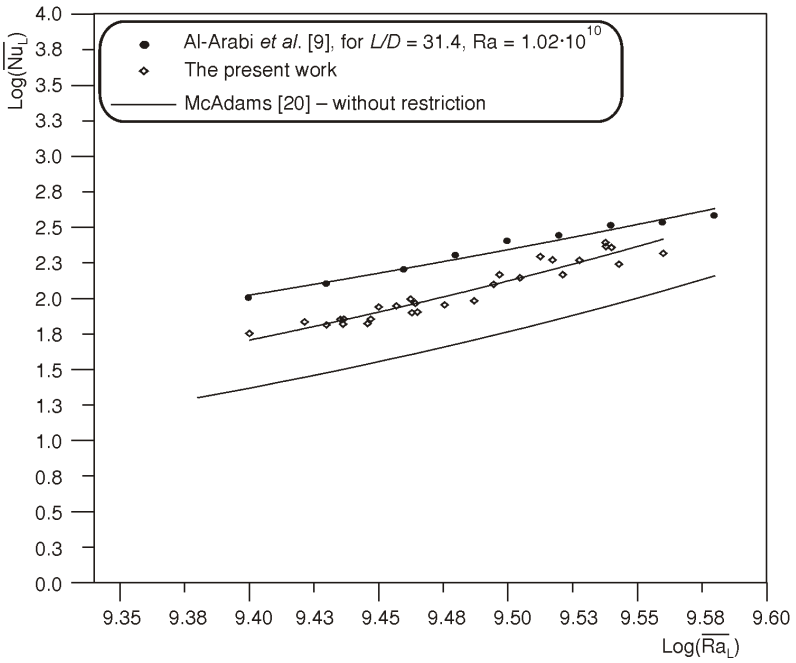

Figure 17. Correlation between the average Nusselt number versus the average Rayleigh number for different inlet configurations

The present results were compared, as shown in fig. 17, with the results of Al-Arabi *et al*. [9] and with vertical cylinder open at both ends without restrictions for laminar flow which it has the following equation as reported by McAdams [20]:

$$\overline{\mathrm{Nu}_\mathrm{L}} \quad 0.59(\overline{\mathrm{Ra}_\mathrm{L}})^{0.25} \tag{28}$$

From the comparison, it is obvious that present results lie lower than Al-Arabi *et al*. [9] because of the higher Rayleigh number range used in his study and it was clear from the comparison with [20] that the different inlet configuration and length has a tremendous effect on the heat transfer results.

Conclusions

As a result from the experimental work conducted in the present investigation to study free convection heat transfer from the inside surface of a uniformly heated vertical circular pipe with different inlet configurations, the following conclusions can be made. The surface temperature increases as the heat flux increases. For the same heat flux the surface temperature for inlet configuration with $L/D = 40$ would be higher than that for

other inlet configurations. The variation of Nu_x with *X/D* for all inlet configurations has the same trend. It was observed that, for all inlet conditions, the Nu_x increases with the increase of heat flux, and for the same heat flux the Nu_x value for bell-mouth would be higher than that for other inlet configurations and the lower value of Nu_x would be occurred in $L/D = 40$. Empirical correlations in the form of $\log\overline{Nu}_L$ against $\log\overline{Ra}_L$ using pipe length as the characteristic linear dimension represent the results for each inlet configurations have been obtained in eqs. (23)-(26). General empirical correlation for all inlet configurations has been proposed, eq. (27), with an overall accuracy of heat transfer data in the order of 8%. The results have been compared with the results of Al-Arabi *et al*. [9] and with McAdams [20]. The comparison shows that the inlet configuration and length has a tremendous effect on the heat transfer results.

Nomenclature

A_s – pipe surface area, [m^2]
c_p – specific heat at constant pressure, [$Jkg^{-1}°C^{-1}$]
D – pipe diameter, [m]
$\underline{Gr}_L$ – local Grashof number based on pipe length (= $g\beta L^3(T_s - T_a)/\nu^2$), [–]
$\overline{Gr}_L$ – average Grashof number based on pipe length (= $g\beta L^3(\overline{T}_s - \overline{T}_a)/\nu^2$), [–]
g – gravitational acceleration, [= 9.81 ms^{-2}]
h – heat transfer coefficient, [$Wm^{-2}°C^{-1}$]
I – heater current, [A]
k – thermal conductivity, [$Wm^{-1}°C^{-1}$]
L – pipe length, [m]
$\underline{Nu}$ – Nusselt number (= hL/k), [–]
$\overline{Nu}_L$ – average Nusselt number based on pipe length (= $\overline{h}L/k$), [–]
Pr – Prandtl number (= $\mu c_p/k$), [–]
Q_{cond} – conduction heat loss, [W]
Q_{conv} – convection heat loss, [W]
Q_{rad} – radiation heat loss, [W]
Q_t – total heat input, [W]
q_{conv} – convection heat flux, [Wm^{-2}]
r – pipe radius, [m]
$\underline{Ra}_L$ – local Rayleigh number based on pipe length (=$\underline{Gr}_L$Pr), [–]
$\overline{Ra}_L$ – average Rayleigh number based on pipe length ($\overline{Gr}_L$ Pr), [–]
T – air temperature, [°C]
V – heater voltage, [V]
x – axial distance, [m]
X/D – dimensionless axial distance, [–]

Greek symbols

β – thermal expansion coefficient, [K^{-1}]
μ – dynamic viscosity, [$kgm^{-1}s^{-1}$]
ν – kinematic viscosity, [m^2s^{-1}]
σ – Stefan-Boltzman constant, [=$5.66\cdot10^{-8}$ $Wm^{-2}K^{-4}$]
ρ – air density, [kgm^{-3}]

Subscripts

a – air
b – bulk
f – film
i – inlet
L – based on tube length
m – mean
s – surface
w – wall
x – local

References

[1] Incropera, F. P., DeWitt, D. P., Fundamentals of Heat and Mass Transfer, 5th ed., John Wiley & Sons Inc., New York, USA, 2003
[2] Meric, R. A., An Analytical Study of Natural Convection in a Vertical Open Tube, *Int. J. Heat and Mass Transfer, 20* (1977), 4, pp. 429-431
[3] Barrow, R. D., Heat Transfer by Free Convection in Open Ended Vertical Duct, 5th International Heat Transfer Conference, *Proceedings*, Tokyo, 1974, Vol. 3, Paper No. NC2.5, pp. 59-63
[4] Kokugan, T., Kinoshita, T., Natural Convection Flow Rate in a Heated Vertical Tube, *Journal of the Chemical Engineering of Japanese, 8* (1975), 6, pp. 445-450
[5] Hess, C. F., Miller, C. W., Natural Convection in a Vertical Cylinder Subject to Constant Heat Flux, *Int. J. Heat and Mass Transfer, 22* (1979), 3, pp. 421-430
[6] Shigeo, K., Adrian, B., Experimental Study of Natural Convection in a Horizontal Cylinder with Different End Temperatures, *Int. J. Heat and Mass Transfer, 23* (1980), 8, pp. 1117-1126
[7] Shenoy, A. V., Natural Convection Effects on Heat Transfer to Power-Law Fluids Flowing under Turbulent Conditions in Vertical Pipes, *Int. Communication in Heat and Mass Transfer, 11* (1984), 5, pp. 467-476
[8] Chang, C. J., Lin, T. F., Yan, W. M., Natural Convection Flows in a Vertical Open Tube Resulting from Combined Buoyancy Effects of Thermal and Mass Diffusion, *Int. J. Heat and Mass Transfer, 29* (1986), 5, pp. 1543 -1552
[9] Al-Arabi, M., Khamis, M., Abd-ul-Aziz, M., Heat Transfer by Natural Convection from the Inside Surface of a Uniformly Heated Vertical Tube, *Int. J. Heat and Mass Transfer, 34* (1991), 4/5, pp. 1019-1025
[10] Abd-el-Malek, B. M., Nagwa, A. B., Group Method Analysis of Steady Free-Convective Laminar Boundary-Layer Flow on a Nonisothermal Vertical Circular Cylinder, *Int. J. Heat and Mass Transfer, 36* (1991), 2, pp. 227-238
[11] Fukusako, S., Takahashi, M., Free Convection Heat Transfer of Air-Water Layers in a Horizontal Cooled Circular Tube, *Int. J. Heat and Mass Transfer, 34* (1991), 3, pp. 693-702
[12] Yan, W. M., Lin, T. F., Theoretical and Experimental Study of Natural Convection Pipe Flows at High Rayleigh Number, *Int. J. Heat and Mass Transfer, 34* (1991), 1, pp. 291-303
[13] Vinokurov, V. F., Volkov, S. V., Martynenko, O. G., Khramtsov, P. P., Shikh, I. A., Some Aspects of Free-Convective Heat Transfer in Eddy Flow through a Horizontal Tube, *Int. J. Heat and Mass Transfer, 36* (1991), 18, pp. 4487-4491
[14] Yissu, W., Laminar Natural Convection in Vertical Tubes with One End Open to a Large Reservoir, *Int. J. Heat Transfer, 56* (1995), 6, Section B, pp. 3411-3428

[15] Kuan-Tzong, L., Fully Developed Laminar Natural Convection Heat and Mass Transfer in Partially Heated Vertical Pipe, *Int. Communications in Heat and Mass Transfer, 27* (2000), 7, pp. 995-1001
[16] Wojciech, T. K., Natural Convection Heat Transfer around Horizontal Tube in Vertical Slot, *Int. J. Heat and Mass Transfer, 43* (2000), 2, pp. 447-455
[17] He, Y. L., Tao, W. Q., Qu, Z. G., Chen, Z. Q., Steady Natural Convection in a Vertical Cylindrical Envelope with Adiabatic Lateral Wall, *Int. J. Heat and Mass Transfer, 47* (2004), 14-16, pp. 3131-3144
[18] Moawed, M., Experimental Investigation of Natural Convection from Vertical and Horizontal Helicoidal Pipes in HVAC Applications, *Energy Conversion and Management, 46* (2005), 18-19, pp. 2996-3013
[19] Holman, J. P., Experimental Methods for Engineers, 7th ed., McGraw-Hill International Inc., New York, USA, 2001
[20] McAdams, W. H., Heat Transmission, 3rd ed., McGraw Hill Company, New York, USA, 1954 (quoted from Holman, J. P., Heat Transfer, 8th ed., McGraw-Hill International Inc., New York, USA, 1997, chapter 7)

Author's addresses:

H. A. Mohammed
University Tenaga Nasional, College of Engineering,
Mechanical Engineering Depatrment
Km7, Jalan Kajang – Puchong, 43009 Kajang, Selangor, Malaysia

Y. K. Salman
Baghdad University, College of Engineering,
Nuclear Engineering Department
Baghdad – Al-Jaderyia, Iraq

Corresponding author H. A. Mohammed
E-mail: hussein@uniten.edu.my

Paper submitted: May 14, 2006
Paper revised: October 20, 2006
Paper accepted: October 25, 2006